Mon. Not. R. Astron. Soc. **000**, 1–13 (2003) Printed 2 February 2008 (MN LATEX style file v2.2)

Variability in black hole accretion discs

A.R. King[1], J.E. Pringle[2,3], R.G. West[1] and M. Livio[3]
[1] *Department of Physics and Astronomy, University of Leicester, Leicester, LE1 7RH, UK*
[2] *Institute of Astronomy, Madingley Rd, Cambridge, CB3 0HA, UK*
[3] *Space Telescope Science Institute, 3700 San Martin Drive, Baltimore, MD 21218, USA*

Submitted: July 2003

ABSTRACT

Observations of accreting systems often show significant variability (10–20 percent of accretion luminosity) on timescales much longer than expected for the disc regions releasing most of the luminosity. We propose an explicit physical model for disc variability, consistent with Lyubarskii's (1997) general scheme for solving this problem. We suggest that local dynamo processes can affect the evolution of an accretion disc by driving angular momentum loss in the form of an outflow (a wind or jet). We model the dynamo as a small–scale stochastic phenomenon, operating on roughly the local dynamical timescale. We argue that large–scale outflow can only occur when the small–scale random processes in neighbouring disc annuli give rise by chance to a coherent large–scale magnetic field. This occurs on much longer timescales, and causes a bright large–amplitude flare as a wide range of disc radii evolve in a coherent fashion. Most of the time, dynamo action instead produces small–amplitude flickering. We reproduce power spectra similar to those observed, including a $1/f$ power spectrum below a break frequency given by the magnetic alignment timescale at the inner disc edge. However the relation between the black hole mass and the value of the break frequency is less straightforward than often assumed in the literature. The effect of an outer disc edge is to flatten the spectrum below the magnetic alignment frequency there. We also find a correlation between the variability amplitude and luminosity, similar to that found in some AGN.

Key words: black hole physics – X–rays: binaries, galaxies: jets

1 INTRODUCTION

Both Galactic and extragalactic accretion–powered X–ray sources display significant aperiodic variability on a wide range of timescales. Similarities in behaviour between the black hole candidate X–ray binaries (BHCs) and the nuclei of Seyfert galaxies (that presumably also harbour central black holes) have been used to suggest that the physical processes occuring in accretion flows around the black holes in these objects are essentially the same, but scaled in some appropriate manner. There are indeed suggestions that such scaling relationships might be used as an estimate for black hole masses (e.g. Vaughan, Fabian & Nandra, 2002; Markowitz et al. 2003). Although X–ray binaries containing neutron stars as the accreting compact objects also exhibit interesting aperiodic, and quasi-periodic, behaviour (see for example the review by van der Klis 1989), we restrict our attention in this paper to black hole accretion discs, partly in the hope that understanding the physics of such accretion flows might be somewhat less complicated, but also because of the interest in scaling between stellar and supermassive objects.

We stress, however, that the processes we discuss in this paper are fully relevant not only to binary X–ray sources and AGN, but to all objects containing accretion discs, such as cataclysmic variables and protostellar objects.

Two main diagnostics are relevant for the variability of these sources. These are the shape of the power spectrum and the amplitude of the variability. Of course, the latter can be deduced from the normalisation of the former (e.g. Miyamoto et al. 1992) and so strictly speaking, these are just two aspects of the same diagnostic.

The best observed black-hole candidate X–ray binary (BHC) is Cygnus X–1. In the low/hard state the normalised rms variability, $\bar{\sigma}$, is of order a few tens of per cent and the power spectrum can be approximated as a broken power law of the form $p(f) \propto f^{-\alpha}$ where $\alpha \simeq 0$ for 10^{-3} Hz $< f <$ 0.1 Hz, $\alpha \simeq 1$ for 0.1 Hz $< f < f_{\rm br} \simeq 3$ Hz, and $\alpha \simeq 2$ for $f_{\rm br} < f < 10^3$ Hz (Nowak et al. 1999; Revnivtsev, Gilfanov & Churazov 2000; Churazov, Gilfanov & Revnivtsev 2001). This implies that the flickering variability occurs

predominantly on timescales in the range 0.3 s – 10 s. In the high/soft state the normalised rms variability, $\bar{\sigma}$, is of the order of a few per cent, and the spectrum is a similar, broken power law, except that now $f_{\rm br} \simeq 10$ Hz, and $\alpha \simeq 1$ for $f < f_{\rm br}$. In this state, therefore, the flickering occurs predominantly on timescales $\gtrsim 10$ s. Other BHCs show similar behaviour. The power spectra of GX339-4 and GS2033+338 in the low/hard state are given by Miyamoto et al. (1992) who note their strong similarity to Cyg X–1. The power spectrum of LMC X–1 is shown by Nowak et al. (2001) to be similar to Cyg X–1 in the high/soft state, and to have a normalised rms variability of $\bar{\sigma} \simeq 7$ per cent.

X–ray power spectra of Seyfert 1 galaxies also typically display a broken power law, with the break occurring at frequency $f_{\rm br} \simeq 10^{-6}$ Hz, corresponding to a timescale of the order of a few days (Markowitz et al. 2003). For $f < f_{\rm br}$ the slope of the spectrum has typically $\alpha \simeq 1$ and for $f > f_{\rm br}$ the slope of the spectrum has typically $\alpha \simeq 2$ (see also Vaughan & Fabian 2003; Vaughan et al. 2003). The normalised rms variability amplitudes range typically up to $\bar{\sigma} \simeq 10$ per cent (Markowitz et al. 2003).

Uttley and McHardy (2001) have drawn attention to a linear correlation between the actual rms variability, σ, and the flux, F, in both BHCs and Seyfert 1 galaxies, implying that the normalised rms variability $\bar{\sigma} = \sigma/F$ is approximately independent of source brightness, at least over a small range in flux. From the data for the BHCs Cyg X–1 and SAX J1808.4-3658, given in the paper by Uttley & McHardy (2001), we find that the relationship is approximately of the form $\bar{\sigma} \propto F^q$ where $q \simeq 0.3$.

The earliest models for the variability were in terms of shot noise (Terrell 1972); the light curves were reconstructed from a series of independent overlapping shots. Such a picture, or variations thereof (e.g. Lehto 1989), can be made to model the data reasonably well, in particular the shape of the power spectrum. However, this scenario still lacks a physical picture for the variability. Since then, various ideas have been put forward, including accretion disc turbulence (Nowak & Wagoner, 1995), magnetic flares in the disc corona (e.g. Poutanen & Fabian, 1999), and MHD instabilities in the plunging region of the inner disc (Hawley & Krolik, 2001). These models all have a common problem in accounting simultaneously for the range of timescales and the normalised rms variability amplitudes. The latter are typically around 10 per cent, and imply emission from the inner few disc annuli, where most of the accretion energy is released (see for example the discussion by Bruch, 1992; Fritz & Bruch, 1998). But these models also imply that characteristic variability takes place on local dynamical timescales. At the inner radii of accretion discs around $\sim 10 M_\odot$ black holes, these relevant timescales are far too short, typically of the order of milliseconds.

An insightful paper by Lyubarskii (1997) offers a way out of these difficulties. Lyubarskii considers small amplitude local fluctuations in the accretion rate at each radius, caused by small amplitude variations in the viscosity, and then considers the effect of these fluctuations on the accretion rate *at the inner disc edge*. A linear calculation shows that if the characteristic timescale of the viscosity variations is everywhere comparable to the viscous (inflow) timescale, and if the amplitude of the variations is independent of radius, then the power spectrum of luminosity fluctuations has the form $p(f) \propto 1/f$. If the amplitude of the variations increases with radius, the slope of the power spectrum of the luminosity variations is steeper than -1. Lyubarskii (1997) notes that he has no physical model for the cause of such fluctuations. In particular, although the obvious candidate cause is the magnetic dynamo, the characteristic timescales for the dynamo are much shorter than the local viscous timescale.

In this paper we use the idea (Livio, Pringle & King 2003) that although the local dynamo timescale at each point in the disc is indeed short, the timescale for the dynamo processes in a sufficient number of independent neighbouring disc annuli to produce a poloidal magnetic field coherent enough to affect the accretion rate, by generating a disc wind or jet, can be quite long. That a disc wind/jet can be a significant driver of accretion in such objects is in line with the recent ideas about 'jet–dominated' states in black hole candidate binaries proposed by Fender, Gallo & Jonker (2003). We propose a specific, but highly simplified, model of an accretion disc. A magnetic dynamo process generates the viscosity, but also, from time to time, produces a sufficiently well–ordered poloidal field. Therefore, the angular momentum is transferred outwards by two separate processes — the usual magnetic viscosity and a disc wind or jet. Numerical simulation of all the physical processes involved in such an intricate system is, of course, unrealistic at the current time, and we make no attempt to describe the full MHD problem in its three–dimensional complexity (e.g. Hujeirat, Camenzind & Livio 2002). Instead, we make a number of simplifying assumptions about the physical processes involved, and use these to construct a numerical description of the time-dependence of such an accretion disc. We show below that this straightforward approach, based on simple physical ideas, can describe the flickering behaviour observed in accreting black hole systems.

2 THE EQUATIONS FOR DISC EVOLUTION

In this Section we derive and explain the equations we use to describe the time evolution of the disc. We simplify the problem by adopting a one–dimensional formulation and using current ideas and simulations to introduce some of the basic physics. We measure disc radii in units of the inner radius $R_{\rm in}$, and assume an outer radius $R_{\rm out}$ large enough (typically $20,000 R_{\rm in}$) that the outer disc can act as a reservoir, allowing the inner disc to approach a quasi-steady state. We avoid undue complexity in these preliminary computations by ignoring the details of internal structure and thermal effects within the disc. Instead, we assume a fixed disc opening angle, with thickness $H \propto$ disc radius R. We typically take $H/R = 0.08$ for numerical convenience: a smaller and perhaps more realistic value would require longer run times, without changing the character of our results. We use a fixed grid with logarithmic spacing. We choose the zone width $DR \simeq H$ and thus $N \simeq 130$ zones. This is not strictly necessary, but gives sufficient accuracy for our current purposes — we note that the main errors in our treatment are likely to come more from our assumptions than from numerical inaccuracy. Indeed, using a formal numerical radial resolution which is finer than the disc thickness, is not likely to have physical meaning. In addition, the convenience of

the choice $DR \simeq H$ becomes apparent in Section 2.2.1. The disc material is assumed to have Keplerian angular velocity $\Omega = (GM/R^3)^{1/2}$ about a central point mass M, and we use units with $GM = 1$. In the present paper we consider a disc extending inwards close to the last stable orbit around the black hole, as is generally thought to occur in the high/soft X–ray state.

2.1 The surface density

We assume that the surface density Σ evolves because of viscous angular momentum transfer within the disc and because of angular momentum loss in the magnetic wind or jet. Note that we use the terms jet and wind simply to mean a mechanism by which the disc can lose energy and angular momentum, without being more specific. Thus we write (Pringle, 1981; Livio & Pringle 1992)

$$\frac{\partial \Sigma}{\partial t} = \frac{3}{R}\frac{\partial}{\partial R}\left[R^{1/2}\frac{\partial}{\partial R}(\nu \Sigma R^{1/2})\right] - \frac{1}{R}\frac{\partial}{\partial R}\left[R\Sigma U_R\right], \qquad (1)$$

where $U_R < 0$ is the radial velocity induced by angular momentum loss in the jet/wind (see Section 2.2.2). Note that we assume that although the jet/wind removes angular momentum from the disc, it does not remove a significant amount of material. It is clear from global energy considerations that the wind cannot remove all of the disc material (put simply, all of the accretion energy cannot go into driving all of the accreting material back to infinity). Hence, at the level of accuracy to which we are working, we neglect mass–loss to the wind in the surface density evolution.

The viscosity ν is assumed to result from magnetic torques generated by dynamo activity within the disc. We use here the standard Shakura-Sunyaev (1973) parametrisation of that viscosity using the dimensionless parameter α in the form

$$\nu = \alpha c_s H, \qquad (2)$$

where c_s is the (appropriately averaged) sound speed in the disc. Using hydrostatic balance we have approximately

$$c_s = H\Omega, \qquad (3)$$

and hence

$$\nu = \alpha H^2 \Omega. \qquad (4)$$

Thus if there is no loss of angular momentum to the wind, (i.e. $U_R = 0$), then the evolution equation is a linear diffusion equation for the surface density Σ. We also note that by using this simple prescription and ignoring the thermal structure of the disc, we have for the time being put aside discussion of the role that hysteresis loops in the (ν, Σ)-plane might play. These are the well-known S–curves which are thought to give rise to the outbursts of cataclysmic variables and X–ray transients, and might well play a role in such systems (e.g. Belloni et al. 1997; Watarai & Mineshige, 2003). In this paper we consider disc instabilities caused by the interaction of viscous and wind torques alone.

We take a zero torque condition $\Sigma = 0$ at the inner boundary $R = 1$, allowing accretion to occur freely through the inner boundary. At the outer boundary we impose a zero radial velocity condition. We use a simple first order explicit numerical scheme, using upwind derivatives for the advective U_R term. The scheme is written so that, except at the inner boundary, disc mass is conserved to machine accuracy.

2.2 The magnetic field

At each point in the disc we postulate a poloidal (vertical) field component B_z generated by the disc dynamo producing the viscosity ν. We assume that this field drives the magnetic wind torques causing the inflow velocity U_R. We assume that the field is advected by U_R, and that it is also able to diffuse through the disc because of the magnetic diffusivity η^* resulting from the dynamo process. We discuss each of these assumptions below when describing their implementation in our disc evolution scheme. They imply an evolution equation for B_z in the form

$$\frac{\partial B_z}{\partial t} = -\frac{1}{R}\frac{\partial}{\partial R}\left(RB_z U_R\right) + \frac{1}{R}\frac{\partial}{\partial R}\left(R\eta^*\frac{\partial B_z}{\partial R}\right) + \mathcal{S}_B. \qquad (5)$$

We should note here that our scheme neglects the advection of magnetic field by the velocity induced by the viscosity ν. The dynamo process generating B_z in random fashion (Section 2.2.1) is an integral part of the process generating viscous torques, and hence viscously driven accretion. This allows diffusion of B_z radially through the disc (Section 2.2.3). But, for unit Prandtl number, the timescales on which B_z varies locally due to the dynamo ($k_d\Omega^{-1}$, where physically we expect $k_d \sim 10$, Section 2.2.1) and due to diffusion between neighbouring disc annuli ($\sim H^2/\eta \sim \alpha^{-1}\Omega^{-1}$, Section 2.2.3) are typically much shorter than the radial viscous diffusion timescale ($\tau_{\rm visc} \sim R^2/\nu$).

At the outer disc boundary we take $B_z = 0$, allowing magnetic flux to diffuse outwards, but preventing inward flux advection. At the inner disc radius we assume zero flux loss through either diffusion or advection. The scheme is written so that poloidal flux is conserved to machine accuracy through the disc, accounting for diffusion through the outer boundary and the dynamo source term.

2.2.1 The source $\mathcal{S}_B$ of B_z

We assume that the source of the local vertical field component B_z is the disc dynamo process driving the viscosity. Specifically we assume that, in this respect, each annulus of the disc of width $DR \approx H$ acts independently of all other annuli. We further assume that each annulus generates large enough fields $B_{\rm disc}$ internal to the disc to produce the pseudo–viscous magnetic torques contained in the α–parameter. That is, we assume (Shakura & Sunyaev 1973)

$$\alpha = \frac{B_{\rm disc}^2}{(\Sigma/2H)\, c_s^2}, \qquad (6)$$

and also that the dynamo process gives rise to a local vertical field B_z of magnitude $\lesssim B_{\rm disc}$. We assume, that for each annulus, B_z can be modeled in terms of a stationary series resulting from a stochastic process. We model this process in terms of the Markoff scheme (e.g. Kendall 1976). This is the simplest linear autoregressive scheme other than a purely random series. In this scheme the n–th member of the series u_n is given in terms of the previous by the relation

$$u_n = -\alpha_1 u_{n-1} + \epsilon_n, \qquad (7)$$

where α_1 is a parameter, which for stability has modulus less than unity, and ϵ_n is a random variable with zero mean.

This scheme produces a Markoff series with oscillations of a more or less regular kind. The mean number of series steps between oscillation peaks is $2\pi/\cos^{-1}[-(1+\alpha_1)/2]$, and the amplitude of the oscillations is such that

$$\mathrm{var}\, u = \frac{\mathrm{var}\, \epsilon}{1-\alpha_1^2}. \tag{8}$$

In our simulations we choose $\alpha_1 = -0.5$, so we expect 3.45 series steps between peaks. We envisage the dynamo process to have some local canonical timescale $\tau_d(R)$. We assume that $\tau_d(R) = k_d\Omega^{-1}$ with $k_d \sim 10$ (e.g. Tout & Pringle 1992; Stone et al. 1996). We therefore apply the Markoff process through the source term $\mathcal{S}$ with the appropriate frequency at each radius so as to give rise to that mean timescale.

We vary the amplitude of the process by adjusting the variance of the term ϵ_n. To do this we use a dimensionless parameter B_s. Then ϵ is chosen to be a random variable in the range $[B_{\max}, -B_{\max}]$. The value of $B_{\max}$ is proportional to B_s and chosen so that if $B_s = 1$ the resulting B_z would, on average, produce a magnetic torque (see 2.2.2) driving an inflow velocity similar to that generated by the viscosity, i.e. ν/R. Thus we take

$$B_{\max}^2 = \frac{3}{2}B_s^2\,\pi\alpha\Sigma\,\frac{H}{R}\,\frac{GM}{R^2}. \tag{9}$$

2.2.2 The jet torque and U_R

We assume that the poloidal magnetic field generates a jet/wind removing angular momentum and energy, but negligible mass, from the disc, and so produces inflow velocity U_R. One way to proceed (cf. Lovelace, Romanova & Newman 1994; Lovelace, Newman & Romanova 1997) would be to assume that the inflow velocity in the disc is simply proportional to B_z^2. However, since the source of the poloidal field is the dynamo process which has a radial scale in the disc of order $\sim H \ll R$ we feel that this is not physically justifiable. Instead, we follow the ideas of Tout & Pringle (1996; see also Livio 1996). They suggest that an inverse cascade driven by disc dynamics and reconnection can transform these small–scale poloidal fields into a global poloidal field smaller in magnitude but larger in scale. The component of the poloidal field with a scale of order $\sim R$ could then produce a magnetically dominated outflow.

To model these ideas in the current simulation we define two quantities

$$\langle B_z\rangle \equiv \frac{\int_{R-\Delta/2}^{R+\Delta/2} B_z R dR}{R\Delta}, \tag{10}$$

and

$$\langle B_z^2\rangle \equiv \frac{\int_{R-\Delta/2}^{R+\Delta/2} B_z^2 R dR}{R\Delta}, \tag{11}$$

where typically we take the range $\Delta \simeq R$. Then the quantity

$$\mathcal{Q}(R) = \langle B_z\rangle^2/\langle B_z^2\rangle \tag{12}$$

is a dimensionless measure of the local coherence of the dynamo-generated field, and is such that $0 \le \mathcal{Q} \le 1$.

We could now simply allow the local magnetic torque to depend on $\langle B_z\rangle$ rather than B_z (cf. also Livio & Pringle, 1992) and assume that it gives rise to an inflow velocity, say V_R, given by

$$V_R = -\frac{\langle B_z\rangle^2 R^{3/2}}{(GM)^{1/2}\pi\Sigma}. \tag{13}$$

However, we must also consider the ability of a poloidal field to launch a wind or jet. Although a sufficiently large–scale poloidal field is probably able to give rise to a wind of some sort, Blandford & Payne (1982) point out that the wind is considerably enhanced if the poloidal field lines make a large angle with the vertical, i.e. if B_R/B_z is large enough (see also Ogilvie & Livio 2001). Such a field configuration results if the inflow velocity is comparable to the speed, $\sim \eta^*/R$, with which vertical field can diffuse outwards through the disc. Here η^* is the effective magnetic diffusivity in the disc, defined below in Section 2.2.3. This effect is discussed by Lubow, Papaloizou & Pringle (1994b) and by Lovelace, Romanova & Newman (1994) who conclude that it can drive strongly time–dependent disc behaviour. These ideas are confirmed by the 'accretion-ejection' events seen in the numerical calculations of Casse & Keppens (2002). Lubow et al. (1994b) suggest that the strength of the wind is a sensitive function of the quantity $X = RV_R/\eta^*$. Lubow et al. (1994b) argue that for a locally isothermal disc the loss from the disc is $\propto \exp(-1/X^2)$, and that for large X the loss timescale is the local dynamical one. In the simulations reported here we do not use the non–analytic function $\exp(-1/X^2)$ (sometimes called the April Fool Function, because, although all its derivatives exist at the origin, it is not equal to its null Taylor series about that point). Instead, for numerical reasons we approximate the sensitivity to X by assuming that the radial velocity driven by the jet/wind obeys

$$U_R = V_R\left(1 + \{f_{\rm LPP} - 1\}\frac{X^2}{X^2+4}\right). \tag{14}$$

Here the parameter $f_{\rm LPP}$, assumed ≥ 1, represents the maximum enhancement to the torque that this effect can achieve. This formula has the behaviour that as $X \to \infty$, $U_R \to f_{\rm LPP}V_R$, and U_R tends to V_R at small X. Note that setting $f_{\rm LPP} = 1$ removes this effect.

2.2.3 The magnetic diffusivity η^*

We assume that the disc dynamo producing the effective viscosity ν also gives rise to an effective magnetic diffusivity η. It seems reasonable to assume that the Prandtl number is of order unity, and thus that $\eta = \nu$. However, if the poloidal field is aligned over a scale of order the radius R then it diffuses through the disc at a rate enhanced roughly by a factor of R/H (van Ballegooijen 1989; Lubow, Papaloizou & Pringle 1994a). Of course, the actual rate at which the poloidal field diffuses through the disc depends on the details of the configuration of the field which we do not attempt to model here. We have argued above that the quantity $\mathcal{Q}$ is a measure of the local coherence of the dynamo–generated field. Thus we approximate these effects by assuming that B_z is subject to an effective magnetic diffusivity η^* acting in the radial direction, where

$$\eta^* = \eta\max(1, \mathcal{Q}R/H), \tag{15}$$

and $\mathcal{Q}$ is defined in equation (12).

3 RESULTS

Even though we have approximated much of the essential physics of a full MHD disc calculation for reasons of simplicity, we nevertheless require a number of parameters to specify our results. These are $\alpha, H/R, B_s, f_{\rm LPP}, k_d = \tau_d(R)\Omega(R)$, and $R_{\rm out}/R_{\rm in}$. The resulting behaviour of what is a highly nonlinear system is sufficiently complicated that we do not attempt, in this paper, to undertake a full survey of parameter space. Rather we content ourselves with fixing most of the parameters. We take $R_{\rm out}/R_{\rm in} = 20,000$ and note that the actual value of this is unlikely to play a significant role provided that it is $\gg 1$. For the runs we discuss below (unless indicated otherwise) we take $B_s = 10$, since this value seems to ensure that typical values of the mean poloidal field, $\langle B_z \rangle$, are large enough to have a noticeable effect on the angular momentum loss, but small enough (factors of a few times less than the disc field $B_{\rm disc}$) to be physically plausible. Similarly, unless stated otherwise, we take $f_{\rm LPP} = 3$, since this value ensures that the physical effect of the jet torque plays some role without being unphysically dominant. We also choose parameters such that $H/R \simeq 0.08$ (see below). We then experiment with varying the remaining parameters α and $k_d = \tau_d(R)\Omega(R)$.

In each run, we start from an initial condition in which the disc surface density is constant at all radii and equal to the arbitrary value of unity ($\Sigma = 1$). [Note that we can do this because ν is independent of surface density, hence the evolution equation (1) for Σ is linear in the absence of wind/jet angular momentum.] We start with vertical magnetic field $B_z = 0$ everywhere, but then take one initial step in the Markoff process at each annulus.

In order to get some idea of observable disc parameters we compute estimates of what we denote as a 'disc luminosity' L_d and a 'wind/jet luminosity' $L_{\rm jet}$, as functions of time. We regard the disc luminosity as some measure of the radiative emission from the accretion flow. However we do not model the conversion of gravitational energy into radiation, and the consequent division of this energy between hard and soft X–ray components. It may be that the instantaneous wind/jet luminosity is generally unobserved, except perhaps when rapid variations give rise to internal shocks in the outflow (see, however, Malzac 2003).

We take the disc luminosity as caused solely by viscous dissipation in the disc, and hence (e.g. Pringle, 1981) take each disc annulus DR to contribute an amount

$$\delta L_d = \frac{9}{4}\nu\Sigma\pi\frac{GM}{R^2}DR. \tag{16}$$

We estimate the rate at which energy is removed from each annulus by the wind/jet from the disc by assuming

$$\delta L_{\rm jet} = (-U_R)\pi\Sigma\frac{GM}{R}DR. \tag{17}$$

Note that these units are arbitrary in the sense that the units for Σ are arbitrary, but that the relative value of the two quantities does have meaning. The total disc and jet/wind luminosities are then obtained by summing these over all the disc annuli, although evidently most of the contribution comes from the innermost radii. In the figures below we present values for these quantities averaged over 10^4 code time units (≈ 10 s for a central black hole of 14 $M_\odot$). We note that for our canonical parameter values of $B_s = 10$ and $f_{\rm LPP} = 3$, the disc and jet luminosities are approximately scaled versions of each other.

We emphasize that we have implicitly ignored the magnetic energy represented by B_z, which is created/destroyed by the dynamo process, and is dissipated by the diffusivity η. One reason for doing this is that we have no proper model for the processes that generate and destroy B_z or that determine its physical scale. However, even when $B_{\rm disc} \sim B_z$, the local energy flow (per unit disc area) into and out of the poloidal field component is of order $Q_{\rm mag} \sim H(B_z^2/4\pi)/\tau_d$ and is therefore less than the rate at which energy is dissipated in the disc by viscous effects (which depends on $\alpha \propto B_{\rm disc}^2$) by a factor of $\tau_d\Omega = k_d \gg 1$. Thus, given the simplifications we have made, neglect of the poloidal energy is reasonable at this level to a first approximation.

We take the unit timescale for the computations so that the orbital timescale at the inner edge ($R = 1$) is 2π. In order to make comparisons with observations more obvious, in the diagrams and in the discussion below we have taken parameters such that $M = 14M_\odot$, and $R_{\rm in} = 6GM/c^2$ so that $R_{\rm in} = 124(M/14M_\odot)$ km and the time unit is $1.016(M/14M_\odot)$ ms. Runs are carried out typically for a time of $1.6 \times 10^7(M/14M_\odot)$ ms.

3.1 Timescales and frequencies

Before presenting the results of some of our simulations we briefly discuss some relevant timescales. Thus, we convert code time units to milliseconds. For central masses other than 14 $M_\odot$ the inverse angular frequency varies as $\Omega^{-1} \propto M^{-1/2}R^{3/2}$, thus from $10^{-3}(M/14{\rm M}_\odot)$ s at the inside, $R = 1$, to approximately $2.8 \times 10^3(M/14M_\odot)$ s at $R = 20,000$. Similarly, the dynamo timescale τ_d, taken equal to $k_d\Omega^{-1}$, varies as $\tau_d \propto M^{-1/2}R^{3/2}$ from a value of $0.01(k_d/10)(M/14M_\odot)$ s at $R = 1$ to a value of $2.8 \times 10^4(k_d/10)(M/14M_\odot)$ s at $R = 20,000$. We define the dynamo frequency as $f_d = \tau_d^{-1}$. The maximum value of this frequency occurs at the inner edge and is equal to $f_d^{\rm max} = 100(k_d/10)^{-1}(M/14M_\odot)^{-1}$ Hz.

The viscous timescale τ_ν is given (e.g. Pringle 1981) by

$$\tau_\nu \approx \Omega^{-1}(R/H)^2\alpha^{-1}. \tag{18}$$

Thus for the value of $H/R \approx 0.08$ (independent of radius) adopted in these calculations, the viscous timescale varies as $\tau_\nu \propto M^{-1/2}R^{3/2}\alpha^{-1}$ from $16(M/14M_\odot)/(\alpha/0.01)$ s at $R = 1$, to $4.5 \times 10^7(M/14M_\odot)/(\alpha/0.01)$ s at $R = 20,000$. For the calculations presented here this means that at times $t \gtrsim 1,000$ s, the central regions of the disc (say, $R \lesssim 20$) where almost all the energy is generated, and where all the "action" is taking place, act as if they were being fed at a steady rate by a disc with unit surface density. The timescale on which magnetic diffusion works is at most the same as the viscous one, and can be less by a factor of up to $R/H \approx 12.6$. With the viscous timescale we can associate a viscous frequency $f_\nu = \tau_\nu^{-1}$. The highest value of the viscous frequency occurs at the inner edge and for the disc parameters we use here is given by $f_\nu^{\rm max} = 0.0625(\alpha/0.01)(M/14M_\odot)^{-1}$ Hz.

The final relevant timescale $\tau_{\rm mag}$ is that for a sufficient number of neighbouring annuli to generate an aligned magnetic field, that significant local energy loss to the jet/wind occurs. This timescale is discussed in Livio, Pringle & King (2003). From our assumptions, the number of zones needed

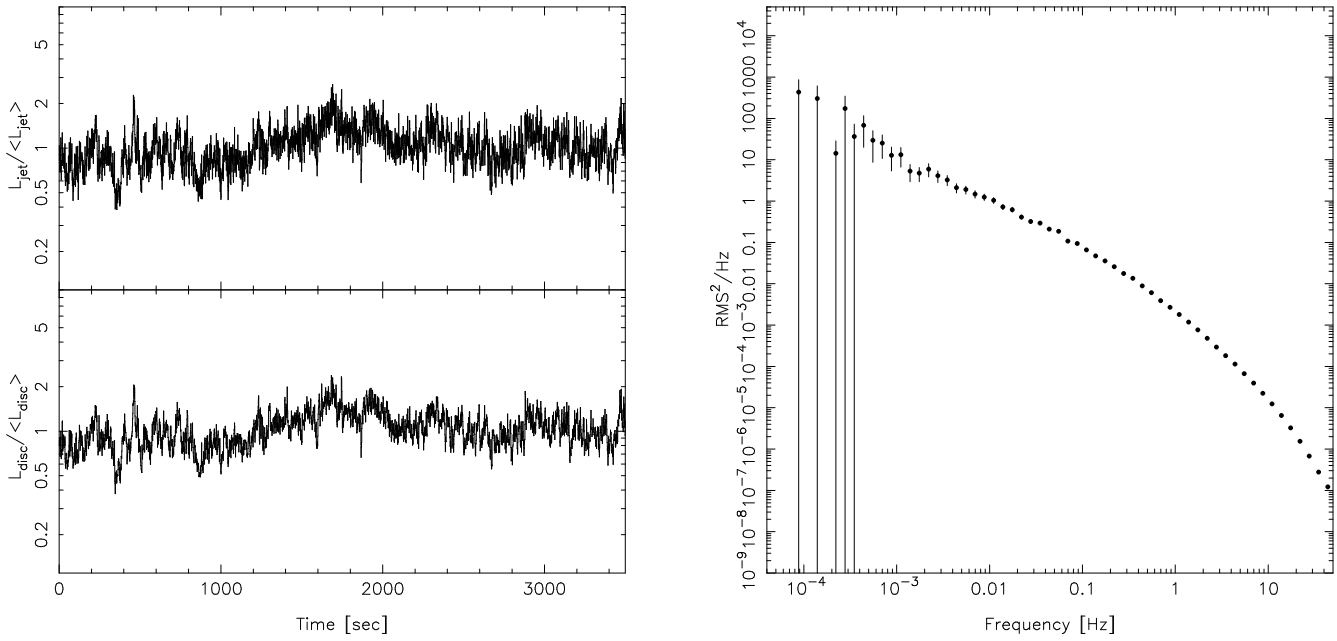

Figure 1. The left panel (a) shows representative jet (top) and disc (bottom) lightcurves for $k_d = 10$, $\alpha = 0.06$. The lightcurves are normalised by the mean luminosity in the segment shown, and binned to 10s time resolution. The right-hand panel (b) shows the disc power spectrum calculated from a 16000s lightcurve. In this and all subsequent figures we give 1σ error bars. $< L_{\rm jet} > / < L_{\rm disc} >= 1.37$ for this case.

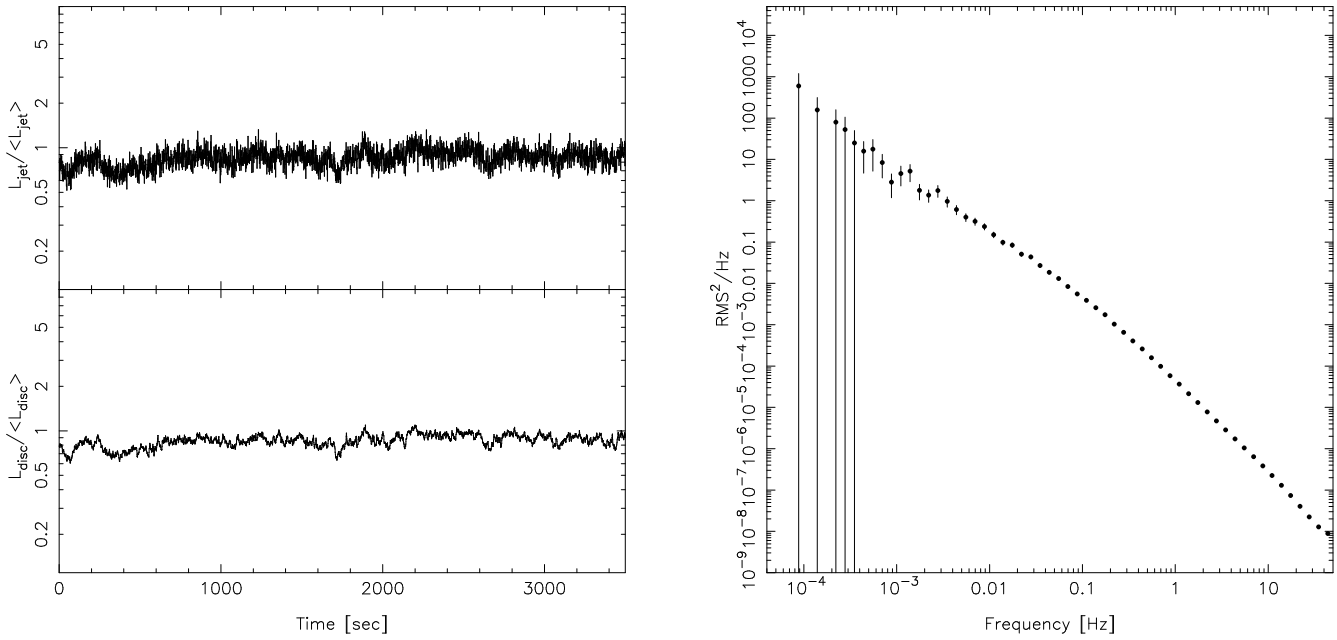

Figure 2. Lightcurves (a, left) and power spectrum (b, right) for $k_d = 10$, $\alpha = 0.006$. Lightcurves have been normalised and binned as per the description of Figure 1. $< L_{\rm jet} > / < L_{\rm disc} >= 3.38$ for this case.

at radius R corresponds to the number of neighbouring annuli, width $\sim H$, required to span a radial scale of order R. Let this number be $\bar{N} + 1$. Then, assuming for simplicity that B_z can take only the values ± 1, if each zone acts independently, the probability of all $\bar{N} + 1$ zones being aligned is $1/2^{\bar{N}}$. To generate a timescale for this we assume that all the zones at radius R are randomly realigned every $\tau_d(R)$.

To give specific examples, for most of the simulations we take the number of grid zones to be $N_{\rm grid} = 130$ which gives $H/R = 0.079 \approx 0.08$ and $\bar{N} = 8$. Thus the timescale on which the innermost 9 zones become aligned is approximately $\tau_{\rm mag} \approx 2.56(k_d/10)$ s. Since $\tau_{\rm mag} \propto R^{3/2}$ the process occurs more slowly at larger radii. Thus we expect the process to be dominated by timescales at the smallest radii, but modulated by longer timescales corresponding to larger radii. The associated magnetic alignment frequency is given

by $f_{\rm mag} = \tau_{\rm mag}^{-1}$. As for the other frequencies the highest magnetic frequency occurs at the inner edge and is given by $f_{\rm mag}^{\rm max} = 0.39(k_d/10)^{-1}(M/14M_\odot)$ Hz.

As noted by Livio, Pringle & King (2003), the quantity $\tau_{\rm mag}$ depends sensitively on H/R. For example, if we consider $H/R = 0.135$ we find $\bar{N} = 4$, and $\tau_{\rm mag}$ is reduced by a factor of 16. However in the numerical method of this paper we use the fact that $DR = H$. Thus, changing H/R would require a different numerical grid, and also change the viscous timescale (for the same value of α). To investigate the effects of changing the magnetic timescale, without altering other parameters, we here simply vary the parameter k_d. Of course in reality k_d is determined by the physics of the disc. This procedure is designed to mimic the effect of changing H/R in a numerically convenient fashion. Accordingly, we have carried out runs spanning the parameter space $0.001 \leq \alpha \leq 0.6$ and $10 \leq k_d \leq 1000$.

3.2 Power spectra

As we noted above, if $k_d = \tau_d\Omega$ is independent of radius, and if, as we have assumed, H/R and α are also independent of radius, then the ratio of the two relevant timescales $\tau_{\rm mag}$ and τ_ν is also independent of radius. Thus we expect our results, appropriately scaled, just to depend on the dimensionless ratio

$$\frac{\tau_{\rm mag}}{\tau_\nu} \sim \frac{2^{R/H}k_d\alpha}{(R/H)^2} \tag{19}$$

where we have used (18) and $\tau_{\rm mag} \sim \tau_d 2^{R/H}$ (Livio, Pringle & King 2003).

The power spectrum calculated for each lightcurve is normalised using the prescription of Miyamoto et al. (1991), namely

$$P_j = \frac{2|S_j|^2}{\mathcal{R}^2 T} \tag{20}$$

where S_j is the Fourier amplitude at frequency f_j, $\mathcal{R}$ is the mean luminosity of the lightcurve, and T the total duration in seconds. We have applied a logarithmic frequency binning to all the PSDs, with $\Delta f/f = 0.1$.

3.2.1 $\tau_{\rm mag} \simeq \tau_\nu$

In Figure 1(a) we show the light curves for $L_{\rm disc}$ and $L_{\rm jet}$ and in Figure 1(b) we show the normalised power spectrum of the disc luminosity for $\alpha = 0.06$ and $k_d = 10$. For these values of α and k_d, $\tau_{\rm mag}(R=1) \simeq \tau_\nu(R=1) \simeq 2.7/(M/14M_\odot)$ s, or, equivalently, $f_{\rm mag}^{\rm max} \simeq f_\nu^{\rm max} \simeq 0.4(M/14M_\odot)^{-1}$ Hz. From Figure 1(b) we see that at frequencies $f \ll f_{\rm mag}^{\rm max} \simeq f_\nu^{\rm max}$ the power spectrum has the form $p(f) \propto 1/f$. This corresponds exactly to the situation described and predicted by Lyubarskii (1997). At each radius the local inflow rate is perturbed randomly with a characteristic timescale which is approximately equal to the local viscous timescale. These perturbations then flow inwards on the local viscous timescale, and when they reach the inner few radii contribute to the total disc luminosity with a fluctuation on that timescale. The fact that the $1/f$ spectrum extends to frequencies as low as $10^{-3}f_\nu^{\rm max}$ implies that contributions to the variability come from radii as large as $R \sim 100$. In Lyubarskii's (1997) model, the power spectrum drops exponentially at frequencies above $f_\nu^{\rm max}$ because his assumed perturbations have no power at frequencies higher than this. He reached this conclusion because, as he remarked, he had no specific physical model for the perturbations. In the model we consider here there are perturbations to the local inflow rate at all timescales down to the local dynamo timescale at the inner disc edge, $\tau_d(R=1)$, corresponding to a frequency of $f_d \simeq 100$ Hz. At frequencies $f \gtrsim f_\nu^{\rm max}$ the only perturbations affecting the disc luminosity are those which take place at radii close to the inner edge where the potential well is deepest. Thus the shape of the power spectrum in this frequency regime depends simply on the power spectrum of the applied random perturbations. From Figure 1(b) it is apparent that in the model presented here the power spectrum steepens for frequencies above about $f_{\rm br} \approx 0.2$ Hz $\approx f_{\rm mag}^{\rm max}$. The spectrum has a slope of $\mathrm{d}\log p/\mathrm{d}\log f = -2$ at $f \approx 2/(M/14M_\odot)$ Hz, and $= -3$ at $f \approx 20/(M/14M_\odot)$ Hz. We see a similar behaviour, suitably scaled in frequency space, for the run with $\alpha = 0.006$ and $k_d = 100$.

3.2.2 $\tau_{\rm mag} \ll \tau_\nu$

We show in Figures 2(a) and 2(b) the light curves and power spectra for a similar model with $k_d = 10$, but now with $\alpha = 0.006$. Thus in this case we have $f_{\rm mag}^{\rm max} = 0.4/(M/14M_\odot)$ Hz $\gg f_\nu^{\rm max} = 0.04/(M/14M_\odot)$ Hz. As mentioned above, we have the ratio $f_\nu^{\rm max}/f_{\rm mag}^{\rm max} = 0.1$ independent of radius. In this case the power spectrum is nowhere of the form $p(f) \propto 1/f$, and indeed is quite well represented by $p(f) \propto 1/f^2$ at all frequencies. We see similar behaviour for the case $k_d = 10$, $\alpha = 0.001$, for which $f_\nu^{\rm max}/f_{\rm mag}^{\rm max} = 0.017$. In this case the magnetic torque fluctuations throughout the disc occur locally much faster than the timescale on which viscous forces can react and inflow can occur. This implies that the magnetically induced variability has only a local effect. Thus the disc luminosity, which is dominated by contributions from the inner regions, is only affected by magnetic torque fluctuations in those inner regions.

3.2.3 $\tau_{\rm mag} \gg \tau_\nu$

In contrast with the above, in Figures 3(a) and 3(b) we show the light curves and power spectra for a similar model, with $k_d = 10$, except that $\alpha = 0.6$. Thus in this case we still have $f_{\rm mag}^{\rm max} = 0.4/(M/14M_\odot)$ Hz, but now $f_\nu^{\rm max} = 4/(M/14M_\odot)$ Hz $\gg f_{\rm mag}^{\rm max}$. In this regime the power spectrum is approximately of the form $p(f) \propto 1/f$ for frequencies $f \lesssim f_{\rm br}$, where $f_{\rm br} \approx 2f_{\rm mag}^{\rm max}$, independent of the value of $f_\nu^{\rm max}$. In the frequency range $f_{\rm br} < f < f_\nu^{\rm max}$, the power spectrum is roughly of the form $p(f) \propto 1/f^2$, and the power spectrum falls off more steeply at higher frequencies $f > f_\nu^{\rm max}$. These findings are also illustrated by the cases $\alpha = 0.06, k_d = 100$ and $\alpha = 0.06, k_d = 1000$ (Figure 4). In this case, because the viscous timescale is short, all magnetic torque fluctuations can be communicated to small radii, and so can contribute efficiently to fluctuations in the disc luminosity. At frequencies lower than about $f_{\rm mag}^{\rm max}$ the situation is still essentially as described by Lyubarskii (1997) and the power spectrum is of the form $p(f) \propto 1/f$. However, at frequencies higher than this, but still below $f_\nu^{\rm max}$, the fluctuations carried inwards to small radii have ever lower amplitudes, so the power spectrum steepens. At frequencies

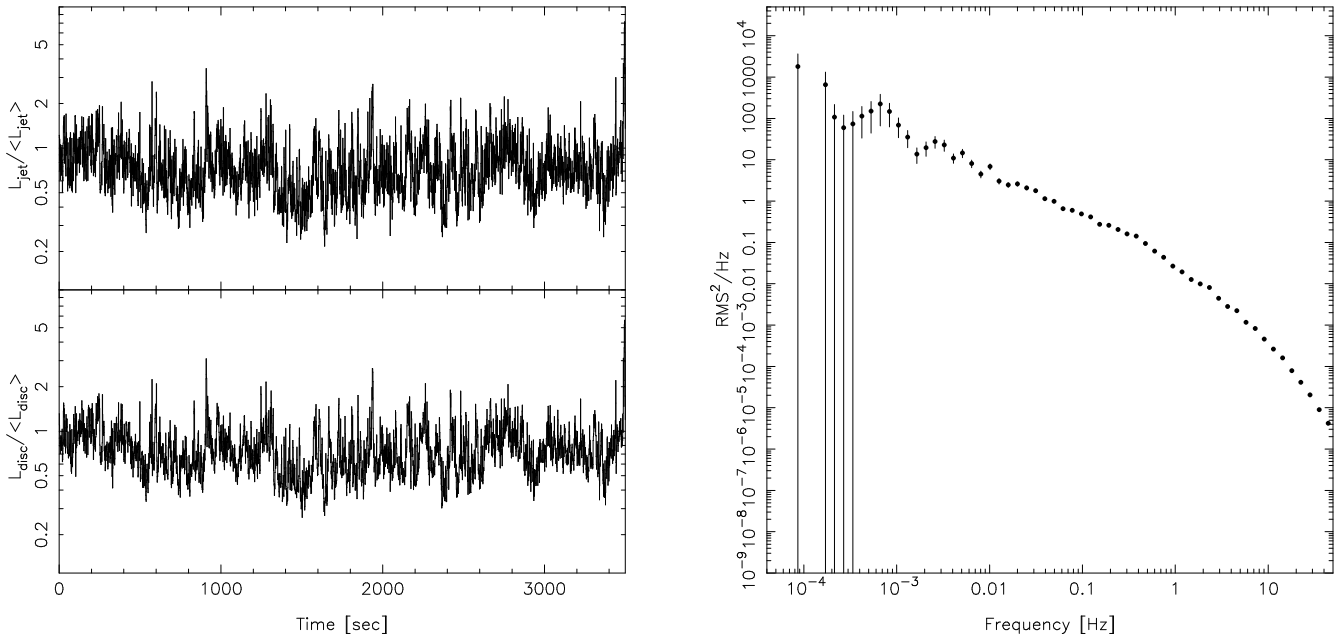

Figure 3. Lightcurves (a, left) and power spectrum (b, right) for $k_d = 10$, $\alpha = 0.6$. Lightcurves have been normalised and binned as per the description of Figure 1. $< L_{\rm jet} > / < L_{\rm disc} >= 0.50$ for this case.

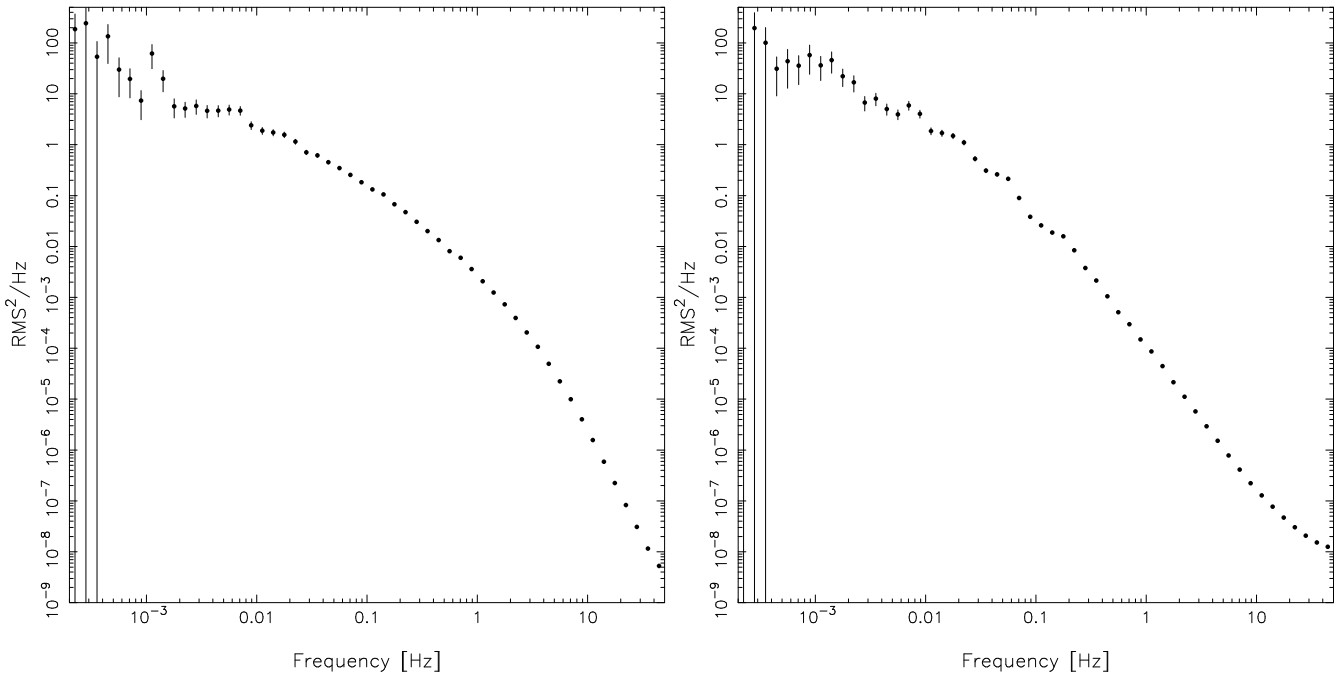

Figure 4. Power spectra for $\alpha = 0.06$, implying $f_\nu^{\rm max} = 0.4$ Hz, and the cases $k_d = 100$ (left) with $f_{\rm mag}^{\rm max} = 0.04$ Hz and, $k_d = 1000$(right) with $f_{\rm mag}^{\rm max} = 0.004$

higher than $f_\nu^{\rm max}$ however, there is no time for fluctuations to be carried inwards from larger radii, and all we see is the effects of local fluctuations occurring in the innermost disc radii. Hence the power spectrum steepens still further.

3.2.4 Effect of the outer disc edge

In the computations presented so far, all the processes have varied with radius in a self–similar manner. Thus, for example, the ratio $f_\nu/f_{\rm mag}$ was independent of radius. For this reason, the structure of the power spectra has been relatively straightforward to interpret. In general, of course, the situation is likely to be more complex, with, for example, both f_ν and $f_{\rm mag}$ being intricate, and different, functions of

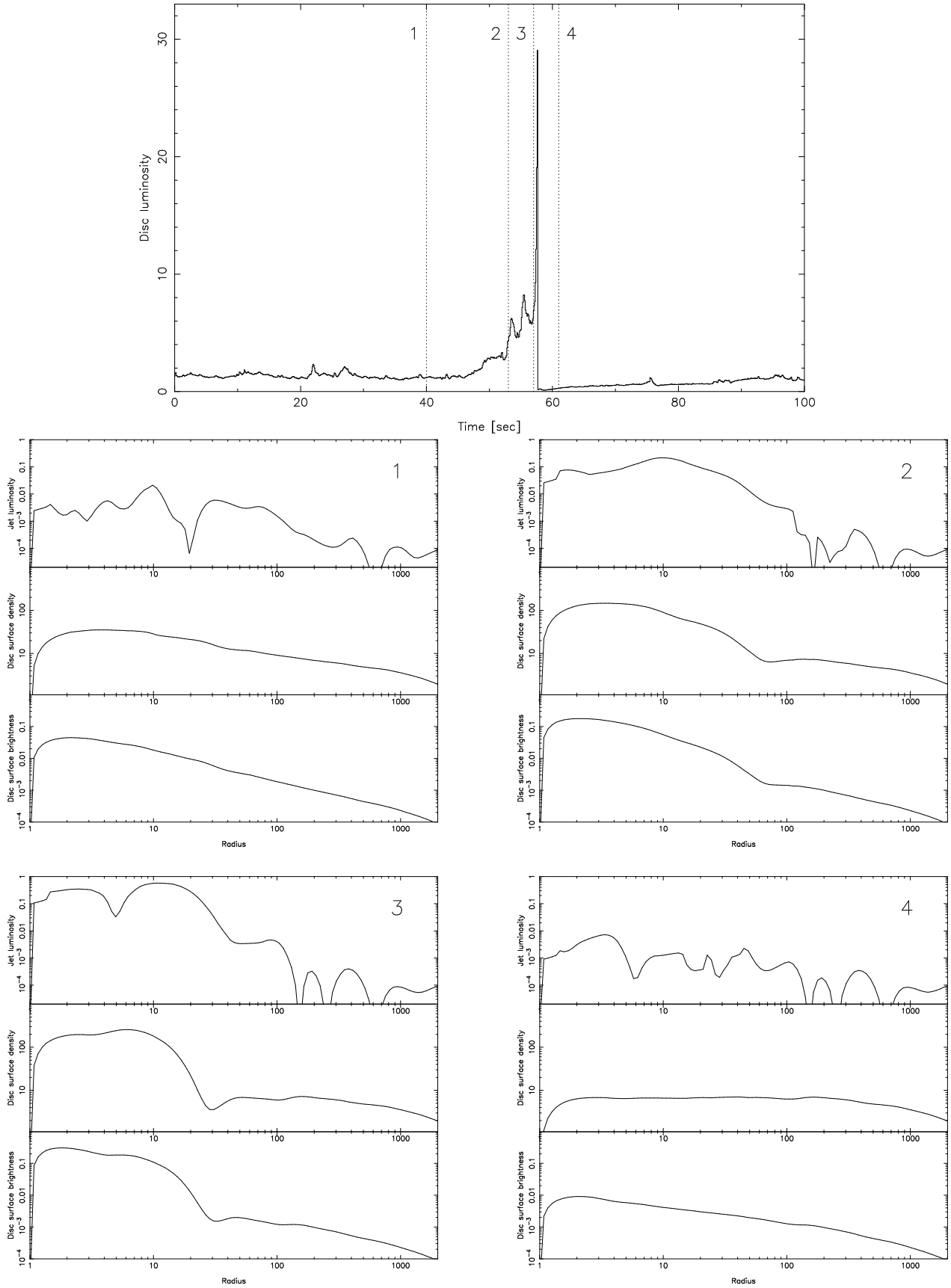

Figure 6. The evolution of the disc and jet throughout a large amplitude flare ($\tau_{\rm d} = 100, \alpha = 0.6$). Four selected times are marked on the lightcurve. The top panel shows the disc lightcurve segment covering the flare event. The four lower panels show the disc surface brightness, surface density and jet luminosity for the four selected times.

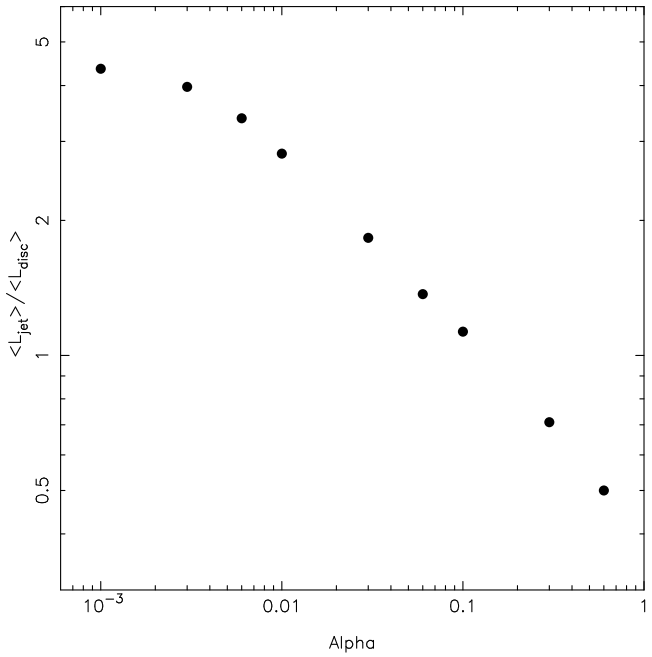

Figure 5. The ratio $< L_{\rm jet} > / < L_{\rm disc} >$ versus the viscosity parameter α, for $k_d = 10$.

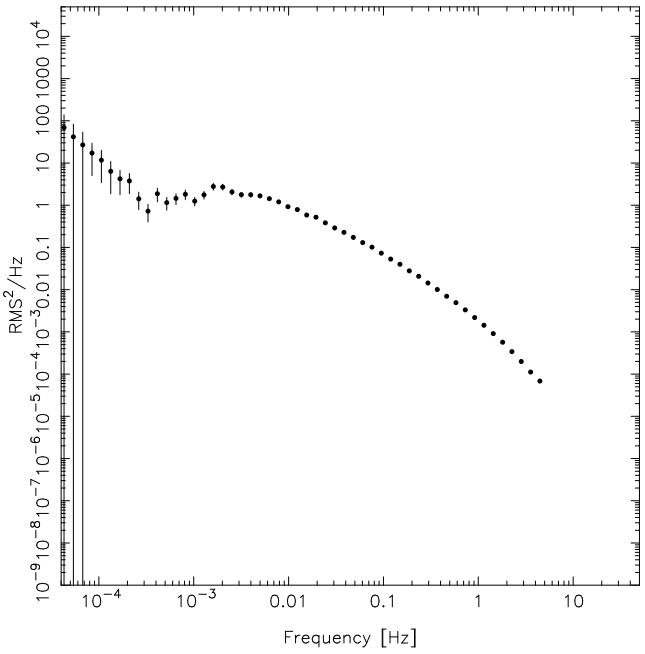

Figure 7. The power spectrum for the case $\alpha = 0.06, k_d = 10$, for which the magnetic wind activity has been turned off at radii $R \geq 100$, corresponding to a frequencies of $f < f_o \approx 0.0013$ Hz.

radius. In this Section we illustrate one simple complication, by setting the dynamo wind activity to zero outside some radius, $R_{\rm max}$. This radius, can be viewed for example as the outer edge of the disc. Alternatively, it can be regarded as a radius outside which the magnetic alignment timescale, $\tau_{\rm mag}$ becomes very long, because the disc thickness suddenly drops outside that radius.

In Figure 7 we show the power spectrum for a run which is identical to that shown in Figure 1 (with $k_d = 10$ and $\alpha = 0.06$), except that dynamo wind activity is turned off for radii $R > R_{\rm max} = 100$. Since we have assumed that the presence of a wind/jet depends on magnetic alignment activity over about a factor of two in radius, we should expect this to give rise to a feature in the power spectrum at a frequency related to $f_o \approx f_\nu(R_{\rm max}/2) = f_{\rm mag}(R_{\rm max}/2) = 0.0013$ Hz. As can be seen by comparing Figures 1 and 7, the effect of truncating wind/jet activity at $R = 100$ is to cause a flattening of the power spectrum from $P(f) \propto 1/f$ to $P(f) \approx$ const. at a frequency $f \approx 0.002$ Hz.

3.3 Lightcurves

In Figures 1 – 3, we have shown some typical samples of lightcurves for both disc and wind/jet emission for $k_d = 10$ and for $\alpha = 0.06, 0.006$ and 0.6. From the Figures it is evident that the disc and wind/jet luminosities follow each other fairly closely, except that the wind/jet emission is much less smooth. This comes about because the wind/jet emission depends directly on the local magnetic field configuration, whereas the disc emission depends on the local disc mass flux which is also mediated by the viscosity.

¿From the simulations we find, as we increase α, that the amplitude of the flickering increases (see Figures 1 – 3). We discuss this in Section 3.3.2 below. We also find that the ratio of average jet luminosity to average disc luminosity decreases (See Figure 5). As can be seen from Figure 5, for the parameters we have chosen $\langle L_{\rm jet}\rangle/\langle L_{\rm disc}\rangle$ is a slowly varying function of α and is unity for $\alpha \approx 0.1$. Since the value of the poloidal field is scaled to ensure that the inflow caused by the wind/jet is on average similar to that caused by the viscosity, it is not immediately obvious what causes this effect. One possibility is that as α increases, keeping the dynamo timescale (measured by k_d) the same, the wind/jet is able to sweep material, and magnetic flux, inwards more efficiently, and therefore to do so at lower values of the poloidal magnetic field.

3.3.1 Large flares

In addition to the continual small-scale flickering shown by our simulated lightcurves, we also see occasional large amplitude flares. In Figure 6 we show an example of one of these, for a run with the parameters $\alpha = 0.6, k_d = 100$. Evidently this flare has a cause similar to that of the small amplitude flickering, except that it is instigated from a much larger radius ($R \sim 100$), is much more coherent, and so is of much larger amplitude. Such large flares, which start at large radius, occur seldom because the timescales at large radii are correspondingly longer. The Figure shows the disc luminosity light curve (we note that the jet luminosity is similar but more spiky), as well as the state of the disc at four particular epochs (marked in the luminosity plot). In these four plots, we note that the disc surface brightness and disc surface density are simply proportional to each other, and are relatively smooth, whereas the jet surface brightness is much more erratic, reflecting the stochastic nature of the local poloidal magnetic field. Box 1 and Box 4 show the disc pre– and post–flare. Comparison of these two Boxes shows that the flare depletes the disc at radii $R \lesssim 100$. The timescale for the recovery of the disc luminosity post-flare indeed corresponds

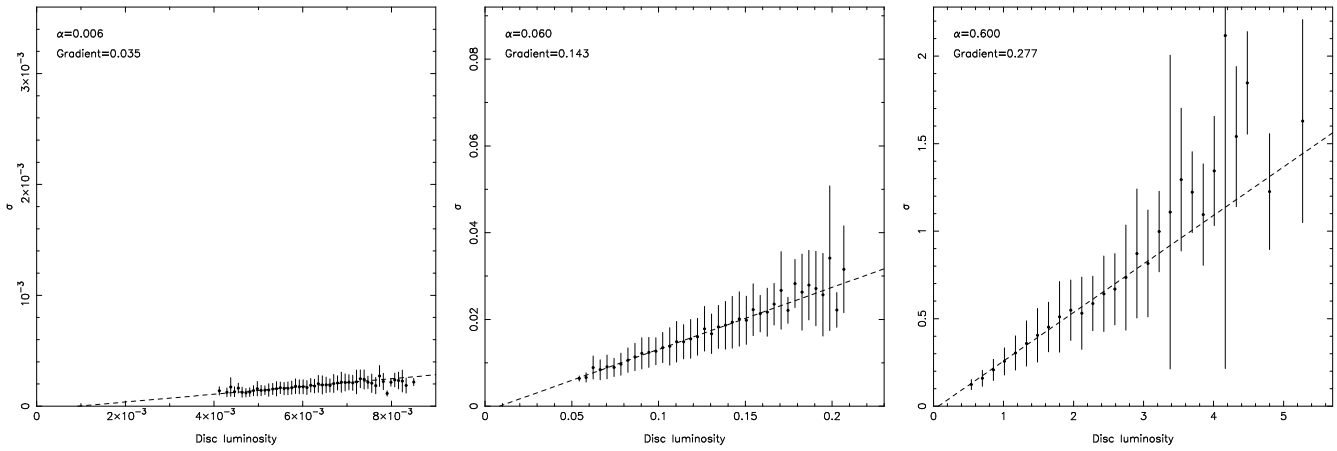

Figure 8. Correlation of the rms variability with flux for three models: $\alpha = 0.006$ (left), $\alpha = 0.06$ (centre) and $\alpha = 0.6$ (right). $k_d = 10$ in all cases.

to the viscous timescale at a radius of $R \sim 100$. We note that observations of GRS 1915+105 (Belloni et al., 1997) show evidence for the viscous refilling of a disc depleted by flares. Box 2 shows the state of the disc at the start of the flare. The incipient dip in surface density at around $R \sim 80$ is the result of a coherent magnetic structure, seen in the jet surface brightness, starting an avalanche of material inwards. Box 3, close to the peak of the flare, shows that this wave of material has moved further inwards, and that the surface density in the inner disc has risen accordingly. We note that this behaviour demonstrates the ability of angular momentum losses in a disc wind/jet to give rise to a wave–like surge of inwardly propagating material, in contrast to the diffusive behaviour of the more usual transfer of angular momentum through viscosity. This can be seen clearly in Equation (1) which governs the evolution of surface density. There, the wind/jet term involving U_R contains a single radial derivative and so is wave-like, or hyperbolic, in character, whereas the viscous term, involving ν has a double radial derivative and so is diffusive, or parabolic, in character. The idea that angular momentum loss to a wind might produce such avalanche/flaring behaviour has been discussed previously by Lubow, Papaloizou & Pringle (1994b), by Lovelace, Romanova & Newman (1994), and by Livio, Pringle & King (2003).

3.3.2 Dependence of flickering amplitude on luminosity

Uttley & McHardy (2001) have shown that in some AGN there is a linear correlation between the amplitude of the flickering and the X–ray flux. To test whether similar behaviour is evident in our model, we divide our lightcurves into 100 second segments and calculate the mean flux ($\bar{F}_j$) and rms flux (σ_j) for the jth segment as follows:

$$\bar{F}_j = \frac{1}{N}\sum_i F_{ij}, \tag{21}$$

and

$$\sigma_j = \frac{1}{N}\sqrt{\sum_i (F_{ij} - \bar{F}_j)^2}, \tag{22}$$

where the index i runs over all time bins in the segment j. The time bins in our lightcurves are 0.1s duration, and thus the σ_j we calculate can be roughly interpreted as the rms variability in the frequency range 0.01 – 10 Hz. The normalised rms variability is then defined as $\bar{\sigma} = \sigma/\bar{F}$.

In Figure 8 we show plots of σ as a function of disc luminosity for the three models whose lightcurves we show in Figures 1 – 3. These have $k_d = 10$ and have $\alpha = 0.006, 0.06$ and 0.6. In each plot the variability amplitude correlates approximately in a linear fashion with the luminosity. The normalised rms variability is then measured by the gradient of this relationship and is therefore roughly a constant for each value of α. Thus, we find that the normalised rms variablity is 3.5 per cent for $\alpha = 0.006$, 14 per cent for $\alpha = 0.06$, and 28 per cent for $\alpha = 0.6$. This increase of normalised rms variability with α is also evident from the power spectra shown in Figures 1 – 3. As was apparent in our discussion of these power spectra, an increase in α leads to an increase in the efficiency with which fluctuations at large radius in the disc are swept inwards to small radii, and thus to an increase in the amplitude of the variability of the disc luminosity, which is produced mainly at small radii.

4 DISCUSSION

Although the disc behaviour we investigate here is relatively complex, one needs to remember that even within the limits of the simple model we have introduced, there are a number of physical processes which we have not addressed, but which are nevertheless likely to play an important role in any observed source.

One major omission is any consideration of the thermal behaviour of the disc. This can have a major impact because the magnetic alignment timescale is a sensitive function of R/H, with $\tau_{\rm mag} \propto \tau_d 2^{R/H}$ (Livio, Pringle & King 2003). This has a number of implications. First, since in most discs the ratio H/R is not a constant, outflow activity is likely to be strong function of radius — for example close to the Eddington limit, the inner parts of the Shakura-Sunyaev disc (1973) have $H \approx$ const. and hence $H/R \propto 1/R$, which would imply enhanced outflow activity in the central disc regions. Indeed, we already know that because jets tend to be

launched mainly from the centres of accretion discs, the outflow behaviour is likely to be strongly non–self similar (See the discussion by Pringle 1993; Livio 1996; Price, Pringle & King 2003). Second, the ratio H/R is in general an increasing function of the accretion rate, or mean disc luminosity. Thus in any given source it is likely that outflow activity, and hence the nature and magnitude of the variability, will depend strongly on the brightness of the source. This effect comes on top of the one presented in Section 3.3.2. Indeed, the data presented by Uttley & McHardy (2001) show some indication that the relation is steeper than linear. Third, a local enhancement of inflow rate caused by outflow activity also leads to enhanced local dissipation within the disc. This leads in turn to a local increase in disc thickness, a marked decrease in $\tau_{\rm mag}$ and thus to enhanced outflow activity. Thus, it seems likely that local outflow activity is significantly self–enhancing. This phenomenon would lead to much more pronounced activity than we find in our current models. Fourth, the thermal hysterisis behaviour which can give rise to outbursting behaviour on its own (as proposed for example for GRS1915+105 by Belloni et al. 1997, and Watarai & Mineshige 2003) could be considerably affected by enhanced outflow behaviour particularly during the hot state when the disc thickness is increased (see also the discussion by Livio, Pringle & King 2003).

Apart from thermal considerations, there are also likely to be further complications which will only come to light when more detailed numerical simulations of the processes involved become possible. One possible effect here is the relationship between the strength of the poloidal magnetic field and the dynamo process. The dynamo process is thought to be driven by the magneto-rotational instability (MRI; Balbus & Hawley, 1991). This instability shuts off if the poloidal field becomes too strong. Suppose then that the dynamo activity at large radius produces (as we have assumed here) a poloidal field sufficient to drive an outflow. This causes wave–like inflow in the disc, carrying with it the poloidal field. As this wave of material moves to smaller radii, the poloidal field becomes advected with it and compressed, this process being mitigated by the effective diffusivity. If at some radius the field becomes strong enough to shut off the MRI, then at that radius both the effective disc viscosity and the effective disc diffusivity are significantly reduced. At that point, the poloidal field is then trapped by the disc, and the wave–like inflow becomes an unstoppable runaway. If this kind of behaviour occurs, then the avalanche-like behaviour we have found in the above models could be a severe underestimate of the violence and frequency of major flaring behaviour.

5 CONCLUSIONS

In this paper we have proposed a simple model to describe how the local dynamo process in an accretion disc, which produces the effective disc viscosity, can also affect the disc evolution by driving angular momentum loss in the form of a wind or jet. While the disc viscosity produces the usual smooth inflow, the accretion rate driven by the wind/jet is highly stochastic. This comes about because of our assumption that efficient angular momentum loss to an outflow can only occur when the local poloidal field produced by the disc dynamo is sufficiently coherent. We assume that each disc annulus (of size comparable to the local disc thickness H) produces a poloidal field whose size and direction varies as a random walk with some characteristic timescale (Markoff process). Only when a number $\sim R/H$ of such neighbouring annuli produce sufficiently aligned poloidal fields can outflow and angular momentum loss occur.

We have implemented these ideas in a simple set of equations that determine the evolution of the disc, and hence the disc and jet(outflow) luminosities. We have chosen the parameters of the model (B_s and $f_{\rm LPP}$) such that the poloidal field strength produced by the disc, while smaller than the tangled field within the body of the disc, is locally large enough to give a significant outflow. Thus, typically, in our models, $L_{\rm jet}$ and $L_{\rm disc}$ are comparable in magnitude. From an observational point of view this is not unreasonable (e.g. Fender et al. 2003; D'Elia, Padovani & Landt 2003). We have chosen simple parameters for our disc models, with constant ratio H/R and constant viscosity parameter α. In addition, we have assumed that local dynamo timescale τ_d is a constant $\times$ the local dynamical timescale Ω^{-1} in the disc. These assumptions imply that the disc is self–similar and that the local viscous timescale τ_ν is proportional to the timescale $\tau_{\rm mag}$ on which the local poloidal field alignment occurs.

We find that in general the disc luminosity shows irregular behaviour. Small amplitude flickering is superposed on variations in the average luminosity, together with occasional large amplitude flares. We have investigated the properties of the flickering with the goal of obtaining an understanding of what the flickering might be able to tell us about the properties of the disc. Lyubarskii (1997) showed that the power spectrum has the form $p(f) \propto 1/f$ if the magnitude of viscosity varies on a timescale everywhere the same as the local viscous time ($\tau_\nu = 1/f_\nu$). In our case the first timescale is that for angular momentum loss in the outflow $\tau_{\rm mag} = 1/f_{\rm mag}$. This is the case shown in Figure 1, where $f_\nu = f_{\rm mag}$. The $1/f$ spectrum continues up to a break frequency $f_{\rm br}$ corresponding to the inner disc edge, beyond which the spectrum steepens. For cases in which the local magnetic alignment timescale was longer than the local viscous time (i.e. $f_{\rm mag} \lesssim f_\nu$) we find a similar behaviour, with the frequency $f_{\rm br}$ corresponding to the local magnetic alignment timescale at the inner disc edge. We do not agree with the assumption found in the literature (e.g. Vaughan & Fabian 2003) that the break frequency corresponds to the viscous timescale at a particular radius. If the local magnetic alignment timescale is everywhere shorter than the local viscous timescale, the spectrum is steeper than $1/f$ throughout (i.e. red noise). We have also shown that the effect of an outer disc edge is to produce a flattening of the spectrum for frequencies $f < f_o$, where f_o is the magnetic alignment frequency at that edge.

We have investigated how the amplitude of the flickering varies with luminosity and with α. We find that in any one run, i.e. at fixed α, the normalised rms amplitude is approximately constant, in line with the findings of Uttley & McHardy (2001) from observation. We also show that the normalised amplitude of the flickering increases with increasing α, varying in our models from about 3 per cent for $\alpha = 0.006$ to almost 30 per cent for $\alpha = 0.6$. This probably comes about because the larger the viscosity, the more

rapidly stochastic behaviour can be swept inwards from the outer disc regions. Thus, it may be that large amplitude flickering is a symptom of a large disc viscosity.

We have also demonstrated the possibility of angular momentum loss to an outflow giving rise to avalanche–like behaviour resulting in a large flare in luminosity. This is because angular momentum loss directly to an outflow changes the characteristic nature of the equation governing the evolution of the disc from diffusive to wave–like. We note that much of the flickering behaviour also comes about because of the wave–like nature of the response. This not only enhances, but also keeps coherent, any perturbations to the disc.

Finally, we stress again that, although we have applied our findings to accretion discs around black holes (BHCs and AGN), the whole range of phenomena found here, and much more (for example, interactions between the disc and the central object's surface and/or its magnetosphere), are likely to occur in all systems in which accretion discs are found.

ACKNOWLEDGMENTS

ARK gratefully acknowledges a Royal Society Wolfson Research Merit Award. RGW is supported by the UK Astrophysical Fluids Facility (UKAFF). JEP gratefully acknowledges continuing support from the STScI Visitors' Program. ML acknowledges support from NASA Grant GO 7378. We thank Drs. P. Jonker and J. Malzac for valuable discussions.

REFERENCES

Balbus, S.A., Hawley, J.F., 1991, ApJ, 376, 214
Belloni, T., Mendez, M., King, A.R., van der Klis, M., van Paradijs, J., 1997, ApJ, 479, L145
Blandford, R.D., Payne, D.G., 1982, MNRAS, 199, 883
Bruch, A., 1992, A&A, 266, 237
Casse, F., Keppens, R., 2002, ApJ, 581, 988
Churazov, E., Gilfanov, M., Revnivtsev, M., 2001, MNRAS, 321, 759
D'Elia, V., Padovani, P., Landt, H., 2003, MNRAS, in press
Fender, R.P., Gallo, E., Jonker, P.G., 2003, MNRAS, in press, astro–ph/0306614
Fritz, T., Bruch, A., 1998, A&A, 332, 586
Hawley, J.F., Krolik, J., 2001, ApJ, 548, 348
Hujeirat, A., Camenzind, M., Livio, M., 2002, A&A Lett., 394, L9
Kendall, M., 1976, *Times Series*, Charles Griffin and Company Ltd, London and High Wycombe, 2nd Ed.
Lehto, H.J, 1989, in *ESA, The 23rd ESLAB Symposium on Two Topics in X–ray Astronomy. Volume 1: X–ray Binaries*, 499
Livio, M., 1996, in *Accretion Phenomena and Related Outflows*, IAU Colloq. 163, eds. D.T. Wickramasinghe, G.V. Bicknell & L. Ferrario (San Francisco: ASP Conf. Ser. 121), xx
Livio, M., Pringle, J.E., 1992, MNRAS, 259, 23P
Livio, M., Pringle, J.E., King, A.R., 2003, ApJ, in press astro–ph/0304367
Lovelace, R.V.E., Romanova, M.M., Newman, W.L. 1994, ApJ, 437, 136
Lovelace, R.V.E., Newman, W.L., Romanova, M.M., 1997, ApJ, 437, 136
Lubow, S.H., Papaloizou, J.C.B., Pringle, J.E., 1994a, MNRAS, 267, 235
Lubow, S.H., Papaloizou, J.C.B., Pringle, J.E., 1994b, MNRAS, 268, 1010
Lyubarskii, Yu.E., 1997, MNRAS, 292, 679
Malzac, J., Belloni, T., Spruit, H.C., Kanbach, G., 2003, A&A, in press, astro-ph/0306256
Markowitz et al., 2003, submitted to ApJ, astro–ph/0303273
Miyamoto, S., Kimura, K., Kitamoto, S., Dotani, T., Ebisawa, K., 1991, ApJ, 383, 784
Miyamoto, S., Kitamoto, S., Iga, S., Negoro, H., Terada, K., 1992, ApJ, 391, L21
Nowak, M.A., Vaughan, B.A., Wilms, J., Dove, J.B., Begelman, M.C., 1999, ApJ, 510, 874
Nowak, M.A., Wagoner, R.V., 1995, MNRAS, 274, 37
Nowak, M.A., Wilms, J., Heindl, W.A., Pottschmidt, K., Dove, J.B., Begelman, M.C., 2001, MNRAS, 320, 316
Poutanen, J., Fabian, A.C., 1999, MNRAS, 306, L31
Price, D.J., Pringle, J.E., King, A.R., 2003, MNRAS, 339, 1223
Pringle, J.E., 1981, ARA&A, 19, 137
Pringle, J.E., 1993, in *Astrophysical Jets*, eds. D. Burgarella, M. Livio & C. O'Dea (Cambridge; CUP), 1
Revnivtsev, M., Gilfanov, M., Churazov, E., 2000, A&A, 363, 1013
Shakura, N.I., Sunyaev, R.A., 1973, A&A, 24, 337
Stone, J.M., Hawley, J.F., Gammie, C.F., Balbus, S.A., 1996, ApJ, 463, 656
Terrell, N.J., 1972, ApJ, 174, 35
Tout, C.A., Pringle, J.E., 1992, MNRAS, 259, 604
Tout, C.A., Pringle, J.E., 1996, MNRAS, 281, 219
van Ballegooijen, A.A., 1989, in *Accretion Disks and Magnetic Fields in Astrophysics*, ed. G. Belvedere (Dordrecht; Kluwer), 99
Uttley, P., McHardy, I.M., 2001, MNRAS 323, 26
van der Klis, M., 1989, ARA&A, 27, 517
Vaughan, S., Fabian, A.C., 2003, MNRAS, 341, 496
Vaughan, S., Fabian, A.C., Nandra, K., 2003, MNRAS, 339, 1237
Watarai, K.–Y., Mineshige, S., 2003, submitted to ApJ, astro–ph/0306548